Available online at www.sciencedirect.com
SCIENCE DIRECT
Polymer 46 (2005) 1865–1877
polymer
www.elsevier.com/locate/polymer

Structural characteristics and properties of silica/poly(2-hydroxyethyl methacrylate) (PHEMA) nanocomposites prepared by mixing colloidal silica or tetraethyloxysilane (TEOS) with PHEMA

Shu-Ling Huang[a], Wei-Kuo Chin[b,*], W.P. Yang[a]

[a]*Department of Chemical Engineering, National United University, Miaoli 360, Taiwan, ROC*
[b]*Department of Chemical Engineering, National Tsing Hua University, Hsinchu 300, Taiwan, ROC*

Received 21 October 2004; received in revised form 22 December 2004; accepted 29 December 2004
Available online 19 January 2005

Abstract

Two methods were used to prepare the silica/poly(2-hydroxyethyl methacrylate) (PHEMA) nanocomposites: one was the direct mixing of colloidal silica with PHEMA using methanol as a co-solvent (colloidal silica/PHEMA) and the other was the adding of the inorganic precursor, tetraethyloxysilane (TEOS), to the PHEMA/methanol solution, followed by the sol–gel process with an acid-catalyst (TEOS/PHEMA). The structure of the colloidal silica/PHEMA hybrid consisted of nano-silica uniformly dispersed in the PHEMA phase with slight inter-molecular hydrogen bonding. The structure of TEOS/PHEMA hybrid was similar to a semi-interpenetrated network with PHEMA chains tethered into the nano-silica network by inter- and intra-molecular hydrogen bonding. Consequently, the TEOS/PHEMA hybrid gels exhibited a smoother surface, higher transparency, and better thermal stability than the colloidal silica/PHEMA hybrid gels.

Keywords: Tetraethyloxysilane; Colloidal silica; Poly(2-hydroxyethyl methacrylate)

1. Introduction

Silica/polymers nanocomposites, a combination of organic polymers and inorganic glass, have received significant much attention in recent years and has been employed in a variety of applications such as optical and nonlinear optical devices [1–4], organically modified ceramic materials [5–8], reinforced elastomers and plastics [9], bioactive glass, chemical/biomedical sensors [10,11] and many others. The silica molecules act as reinforcing agents, making the polymers harder, giving them more compressive strength, improving their heat distortion temperature (HDT), and lowering the coefficient of thermal expansion (CTE). They also reduce the brittleness of pure inorganic glass and help to avoid the problem of stress cracking during the drying process when the inorganic glass blends with the polymeric molecules.

Many studies have been devoted to the preparation of the silica/polymers hybrid materials with organic monomers and inorganic precursors such as tetramethyloxysilane (TMOS) or tetraethyloxysilane (TEOS) through in situ, acid-catalyzed sol–gel processes [12–23]. In these hybrids, the inorganic molecules and organic molecules interconnect by chemical covalent bonds, hydrogen bonds or physical interaction. The structure of the hybrid, either with the nano-silica uniformly dispersing in the polymer phases or with phase separation of inorganic and organic phases occurring, depends on the processing conditions such as the type of catalyst, the pH value, the water quantity, the solvent system, and the reaction temperature [24]. The presence of organic monomers may retard the hydrolysis and condensation reactions of silanols during the sol–gel process [25,26]. Moreover, the low degree of polymerization of organic monomers, due to the effect of chain transfer with alcoholic solvents, reduces the thermal resistance and the strength of the hybrids. Some silica/acrylic polymer hybrids show the yellowish phenomenon caused by the remaining initiators or un-polymeric monomers in the final products [27]. These

* Corresponding author. Tel.: +886 35713721; fax: 886 35715408.
E-mail address: wkc@che.nthu.edu.tw (W.-K. Chin).

0032-3861/$ - see front matter © 2005 Elsevier Ltd. All rights reserved.
doi:10.1016/j.polymer.2004.12.052

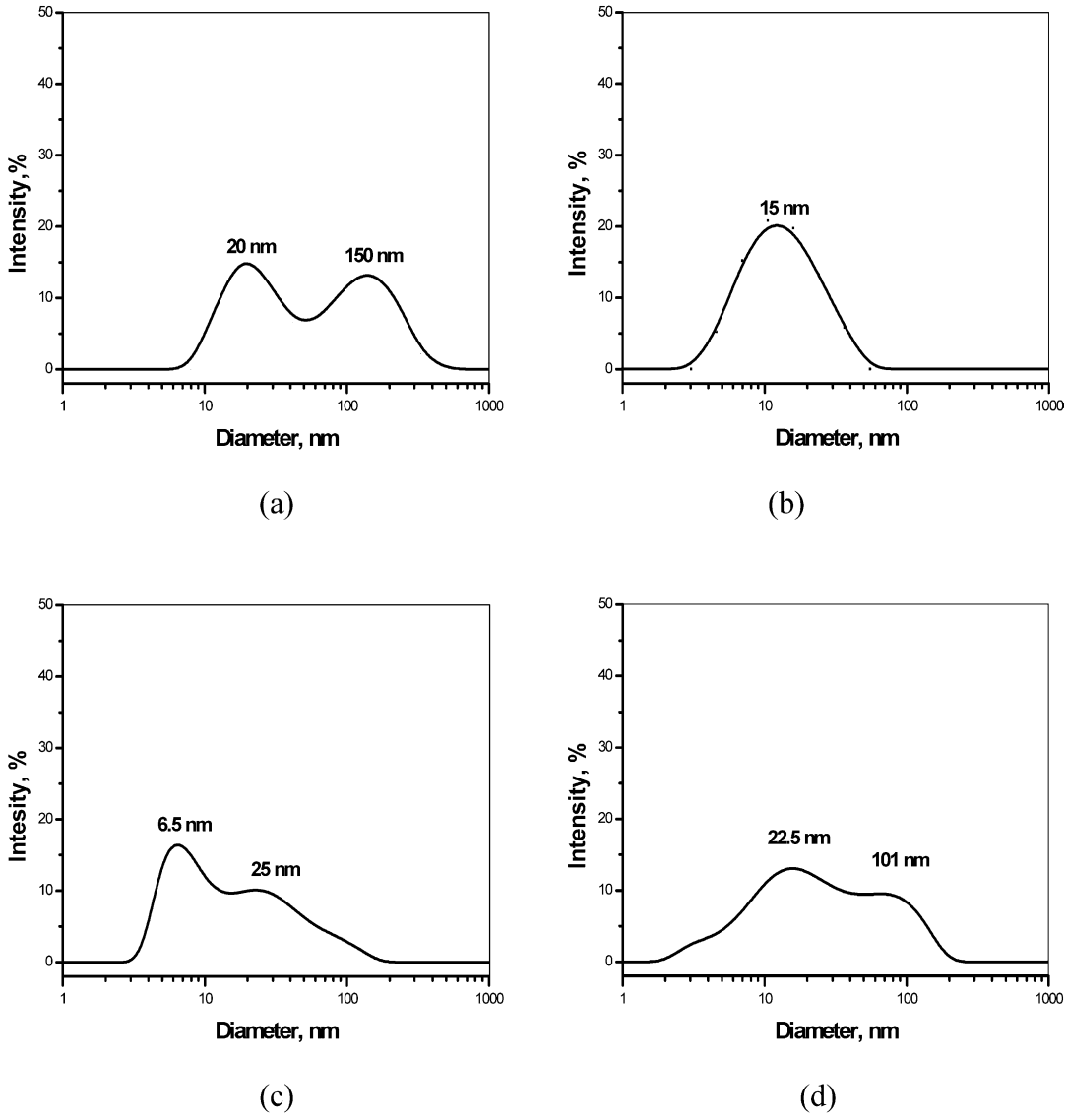

Fig. 1. The particle size distributions of silica in colloidal silica/PHEMA sols. Colloidal silica content: (a) pure colloidal silica, (b) 10 wt%, (c) 30 wt% and (d) 50 wt%.

defects must be avoided, especially in the application of optical materials.

An alternative way to synthesize the inorganic/organic hybrids is by directly mixing inorganic colloidal particles with polymers. Not only can the above-mentioned disadvantages be avoided then, but it also simplifies the preparation process of the inorganic/organic hybrid. The inorganic colloidal particles can be pre-produced through the sol–gel process with a pure inorganic precursor such as alkoxysilanes with base-catalyst conditions as reported in a previous paper [26]. However, there has always been uncertainty about the reinforcement effect of composites prepared by the physically mixing inorganic particles and polymer. Therefore, two methods to prepare the silica/poly(2-hyrdoxylethyl methacrylate) (PHEMA) hybrid gels were used in this study: the direct mixing of the colloidal silica with PHEMA polymer and the mixing of tetraethyloxysilane (TEOS) with PHEMA (followed by the sol–gel process). The structural difference, thermal resistance and light transmittance of hybrids prepared by both methods were evaluated and discussed.

2. Experimental

2.1. Materials

The inorganic precursors, TEOS, and colloidal silica (suspended in an isopropyl alcohol solvent), were obtained from Aldrich Chemical Co. (United States) and the chemical system research division of the Chung-Shan Institute of Science and Technology (Taiwan), respectively.

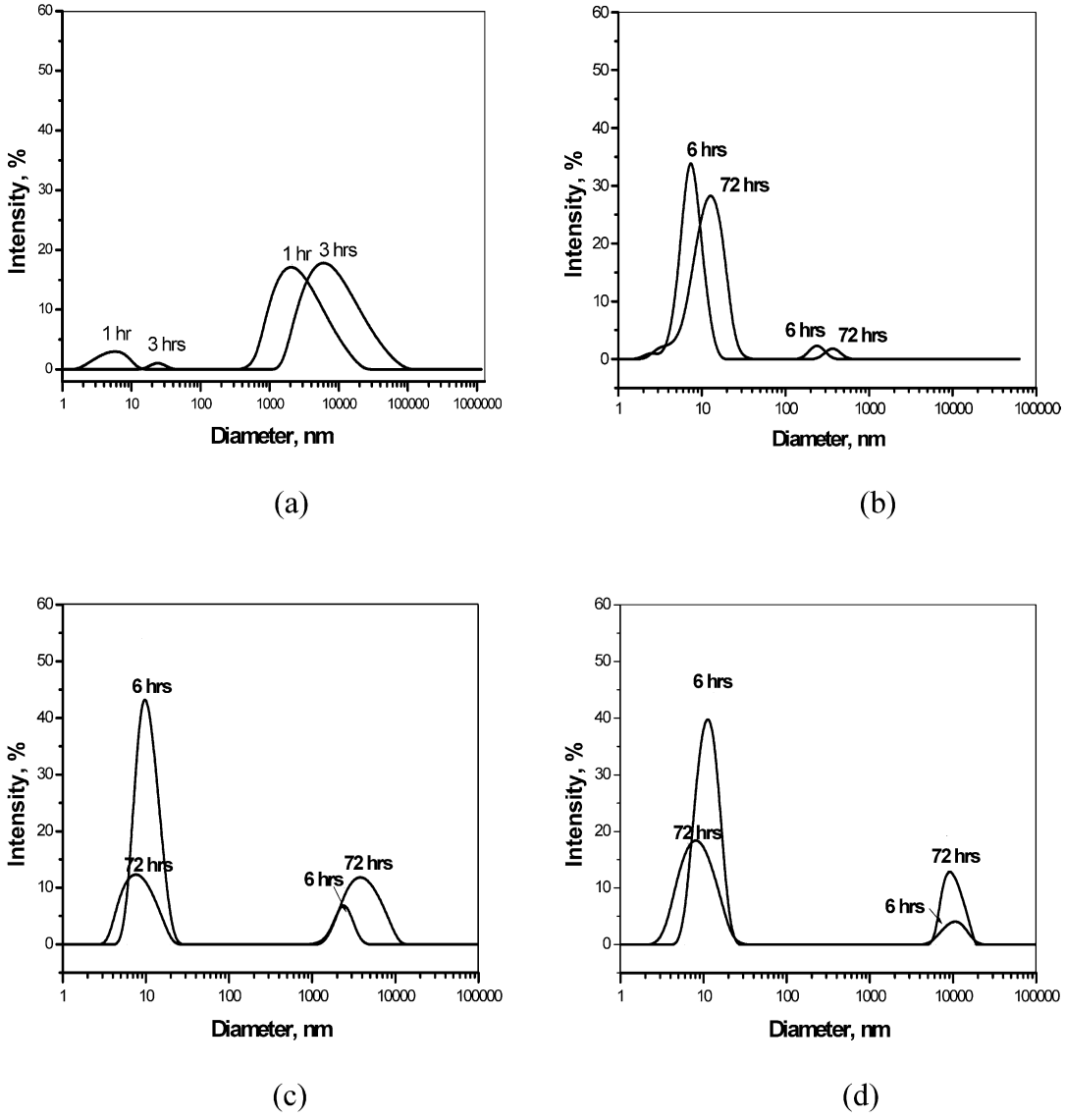

Fig. 2. The particle size distributions of silica in TEOS/PHEMA sols during the sol–gel process under HCl_{aq}-catalyzed condition. TEOS content: (a) pure TEOS, (b) 10 wt%, (c) 30 wt% and (d) 67 wt%.

PHEMA with a molecular weight of 3×10^5 was obtained from the Aldrich Chemical Co. (United States). All aqueous solutions were prepared using de-ionized water.

2.2. Preparation of silica/PHEMA hybrid gels

In the colloidal silica/PHEMA system, the PHEMA was dissolved in the methanol (MeOH) by a weight ratio of 1/8. Various amounts of colloidal silica sol were added to the PHEMA/MeOH solution and mixed in a sealed container for 6 h at 60 °C, then poured into an aluminum mold and dried at 70 °C/24 h plus 105 °C/24 h to vaporize the solvent and water.

The TEOS/PHEMA system consisted of the TEOS precursor dissolved in the aqueous HCl solution with the pH and the molar ratio of H_2O/TEOS fixed at 1.03, and 8, respectively. Various ratios of the PHEMA/MeOH and the TEOS/HCl_{aq} mixtures were stirred for 1 h at room temperature then poured into a sealed reactor and allowed to react at 60 °C for 72 h. During the reaction period, a small portion of the reactant mixture was taken from the reactor to monitor the size distribution of the polymerized silica particles. After the sol–gel reaction was completed, the mixture was removed from the reactor and poured into an aluminum mold, then dried at 70 °C/24 h plus 105 °C/24 h to vaporize the solvent and water.

2.3. Particle sizing analysis

The polymerized silica particle size and distribution were measured by the dynamic light scattering analysis method using a DynaPro-LSRTC molecular sizing instrument

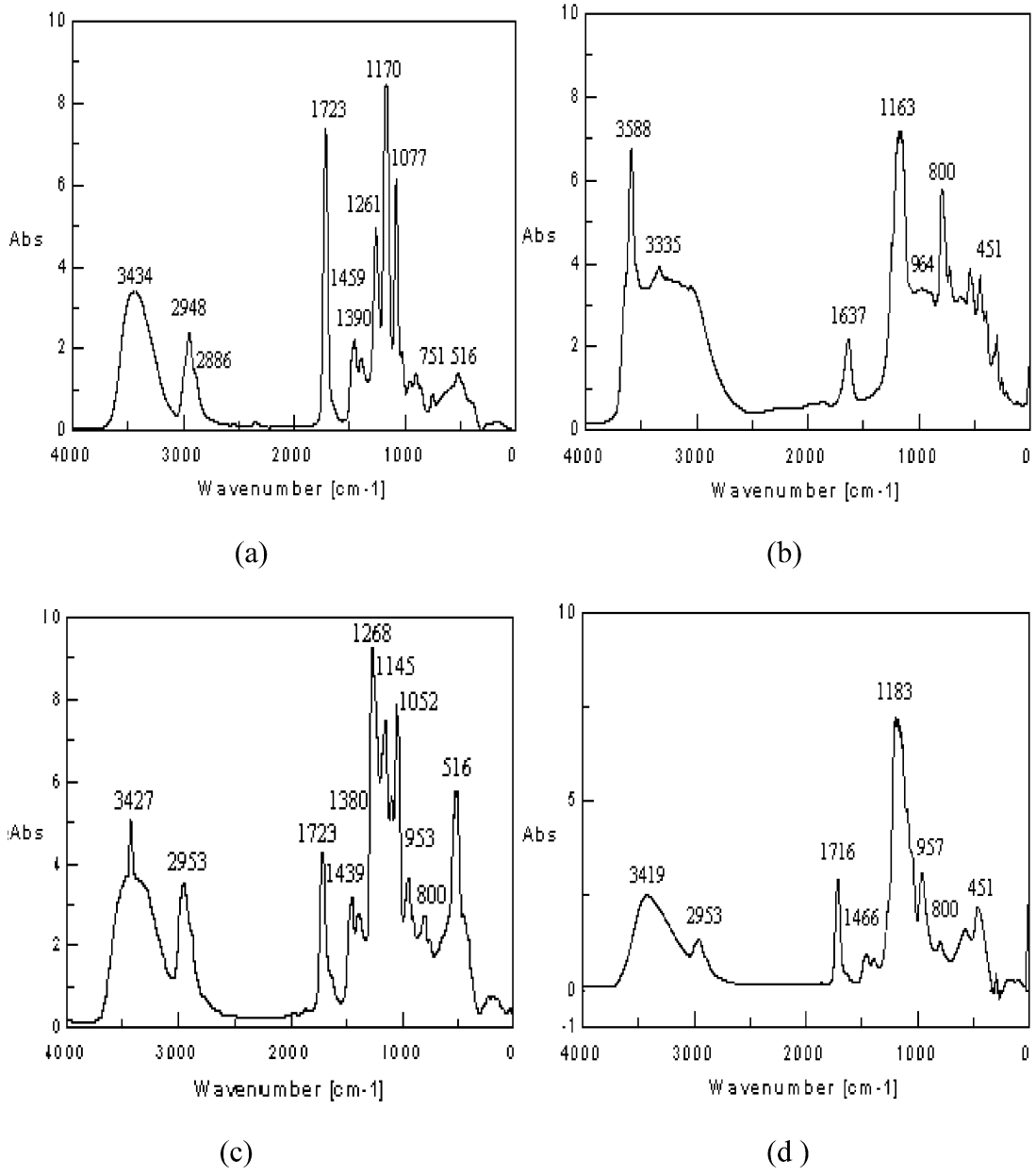

Fig. 3. FT-IR spectra of (a) pure PHEMA, (b) pure silica, (c) colloidal silica/PHEMA hybrid gel containing 30 wt% colloidal silica and (d) TEOS/PHEMA hybrid gel containing 30 wt% TEOS.

(LSRTC, United States) at 25 °C. A 4 ml sol solution was injected into the quartz cuvette and illuminated by an 830 nm solid diode laser with the configuration of a 90° scattering angle.

2.4. Thermal analyses

The thermogravimetric (TGA) analyses of the dried gels were performed with a TGA 951 (DuPont Instruments, United States), under a nitrogen atmosphere at a heating rate of 10 °C/min. The thermal expansion behavior of the hybrid film was measured with a TMA 2940 (TA Instruments, United States) in a nitrogen atmosphere in film clamp mode. A constant load of 0.1 N and the heating rate of 5 °C/min were applied in the TMA analysis.

2.5. Dynamic mechanical analysis

Dynamic mechanical properties, including the storage modulus and damping (tan δ), of pure PHEMA and silica/PHEMA hybrids were obtained with a Q800 Dynamic Mechanical Analyzer (DMA) (TA Instruments, United States) in film clamp mode. The film sample with typical dimensions of $15\times6\times0.5$ mm^3 was prepared through cast

Table 1
Characteristics of IR absorptions in the PHEMA and silica

Vibration[a]	Region (cm^{-1})
PHEMA	
ν (O–H)	3434
δ (O–H)	1261
ν_a,ν_s (CH_2, CH_3)	2948; 2886
δ (CH_2), δ_a (CH_3)	1459
ν (C=O)	1723
CH_2 twist and rock	1390
ν (C–O–C)	1077
ν_a (C–O–C)	1170
ν (–C–O–)	751
Silica	
ν (Si–OH)	3588; 964
ν_a (Si–O–Si)	1163; 800
ν_s (Si–O–Si)	451

[a] ν: stretching vibration, δ: bending vibration, ν_s: symmetric vibration and ν_a: antisymmetric vibration.

molding. The heating rate and frequency were 5 °C/min and 1 Hz, respectively, and the scanned temperature ranged from −50 to 200 °C.

2.6. Fourier transform infrared spectroscopy (FT-IR) analysis

The structural characteristics of the raw materials and hybrid gels were analyzed with an FT/IR-470 FTIR spectrometer (Jasco, United States) in the absorption mode ranging from 400 to 4000 cm^{-1} with a 4 cm^{-1} resolution.

2.7. Surface morphology of hybrid gel

The atomic force microscopic (AFM) images of the silica/PHEMA hybrid gels coated on a silicon wafer were collected by a scanning probe microscopy (Digital Instrument, NS3a-controller with D3100 stage, United States) in contact mode.

2.8. Optical transmittance analysis

The sols, close to the gelling point, were taken out of the reactor and cast in a transparent cell with a casting thickness of about 1 cm; they were then dried at 70 °C. The optical transmittances of the hybrid gels were measured by a U-2001 ultraviolet spectrophotometer (Hitachi Co., Japan) with wavelengths ranging from 300 to 800 nm.

3. Results and discussion

3.1. Evolution of the silica particles in the colloidal silica/PHEMA and TEOS/PHEMA sols

Fig. 1 illustrates the particle size distribution of pure colloidal silica and colloidal silica/PHEMA sols with colloidal silica content ranging from 10 to 50 wt%. The particle size distribution in the pure colloidal silica sol ranged from 7 to 600 nm with two intensive peaks at 20 and 150 nm. The size of the silica particles became smaller while the colloidal silica sol mixed with the PHEMA/MeOH solution. This result implies that the addition of PHEMA and methanol in the sol caused the original cluster–cluster or particle–particle aggregated colloidal silica to be slightly disaggregated.

Fig. 2 shows the evolutions of the silica particles during the sol–gel process of the pure TEOS and TEOS/PHEMA sols with the TEOS content ranging from 10 to 67 wt%. In the pure TEOS sol, the growth of silica particles during the sol–gel transition showed a bimodal size distribution in the range of nanometers and micrometers, respectively. While the reaction time was longer than 3 h, the size of the silica particles was either too large or networks were formed, thus exceeding the measuring limit of the DynaPro molecular sizing instrument. When the PHEMA and methanol were added to the TEOS sol, the enhanced esterification and depolymerization reactions of the silanols as well as the dilution of the concentration of silanols in the sol retarded the growth of the silica particles and finally formed colloidal silica with a bimodal size distribution. In the TEOS/PHEMA sol with a TEOS content of 10 wt%, most of the growing particles were in the range of 2–40 nm. A few particles were in the range of 150–600 nm. Increasing the TEOS content in the hybrid sol, the major portion of growing silica particles remained in the range of 2–30 nm; however, a few particles grew and aggregated to a large size, close to a micrometer with their portion slightly increasing as the reaction time extended from 6 to 72 h.

3.2. FT-IR characterization

The structural difference between the synthesized colloidal silica/PHEMA and the TEOS/PHEMA hybrid gels was measured by FT-IR spectroscopy. Fig. 3 shows the FT-IR spectra of the pristine PHEMA, pure silica and both types of hybrid contained 30 wt% of colloidal silica and TEOS precursor. The group assignments of the IR absorption bands for the PHEMA and the pure silica are summarized in Table 1 [17,23,26]. In the pure silica, besides the absorptions corresponding to the Si–O–Si and Si–OH groups, an absorption corresponding to the H–O–H bending vibration, 1637 cm^{-1}, was also found indicating that residual intra-molecular waters existed within the silica. The colloidal silica/PHEMA hybrid gel was prepared by physically mixing colloidal silica and PHEMA. Hence, its IR spectrum was simply a combination of the IR spectra of silica and PHEMA. In the TEOS/PHEMA hybrids, the tether between the silica and PHEMA chains caused the band absorptions to correspond to the C–OH and C–O–C groups in the PHEMA chains and the Si–O–Si groups in the silica significantly overlapped and, as shown in the band

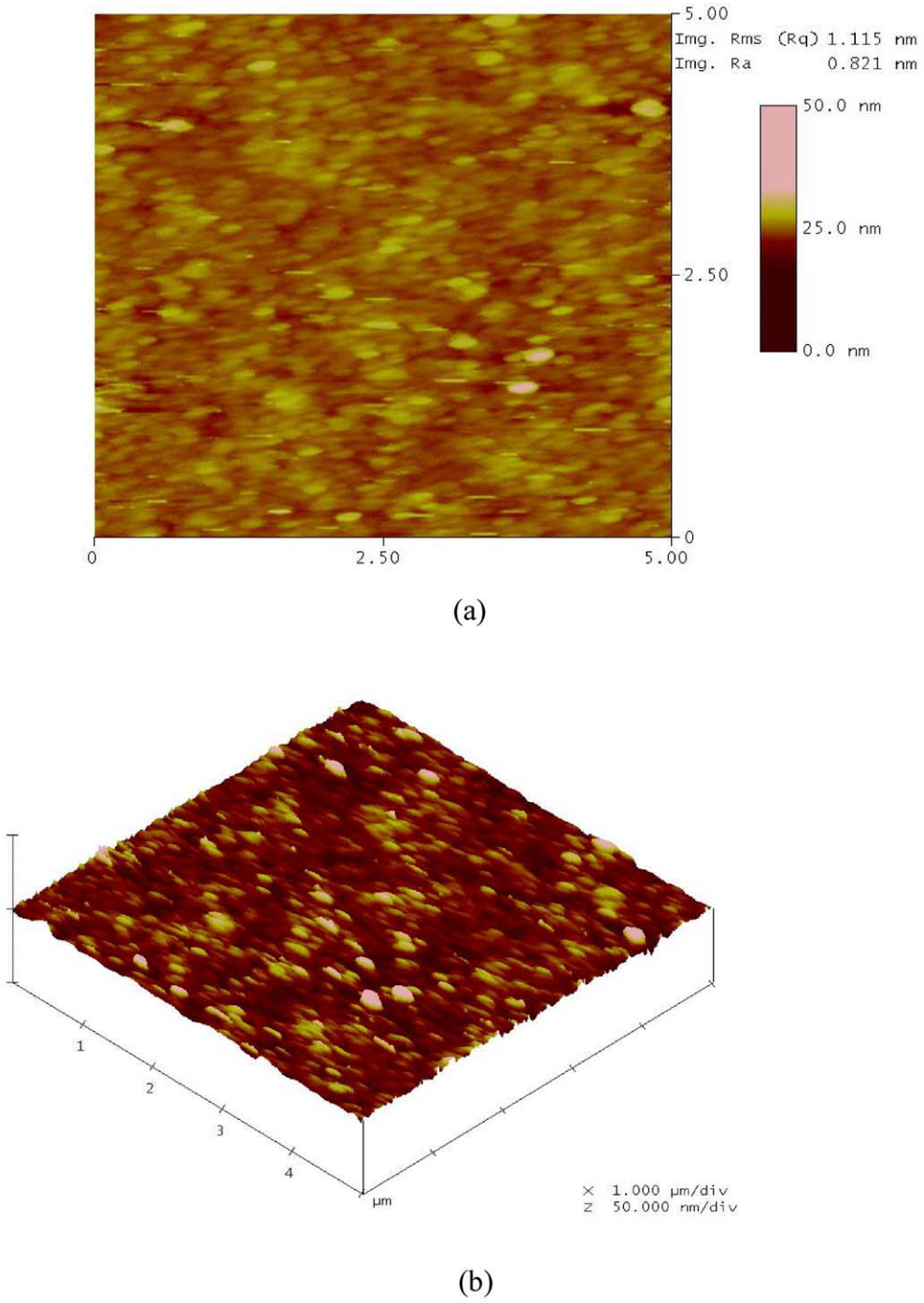

Fig. 4. The AFM images of colloidal silica/PHEMA gel with 30 wt% colloidal silica. (a) Two-dimensional and (b) three-dimensional.

range of 1300–1000 cm^{-1} in the IR spectrum of TEOS/PHEMA hybrid gel, could not be clearly distinguished. In addition, the absorption represented in the hydrogen bonding between the silica and PHEMA chains was slightly different in the colloidal silica/PHEMA and TEOS/PHEMA hybrids. The peak corresponded to the stretching vibration of the hydroxyl groups shifting from 3434 cm^{-1} in the pure PHEMA to 3427 and 3419 cm^{-1} in the colloidal silica/PHEMA and TEOS/PHEMA hybrids, respectively. Also, due to the effect of the intra-molecular hydrogen bonding, the peak of the C=O stretching vibration shifted from 1723 cm^{-1} in the pure PHEMA to 1716 cm^{-1} in the TEOS/PHEMA hybrid. From the difference in the IR spectra between the colloidal silica/PHEMA and the TEOS/PHEMA hybrids it could be concluded that only minimal inter-molecular hydrogen bonding existed between the

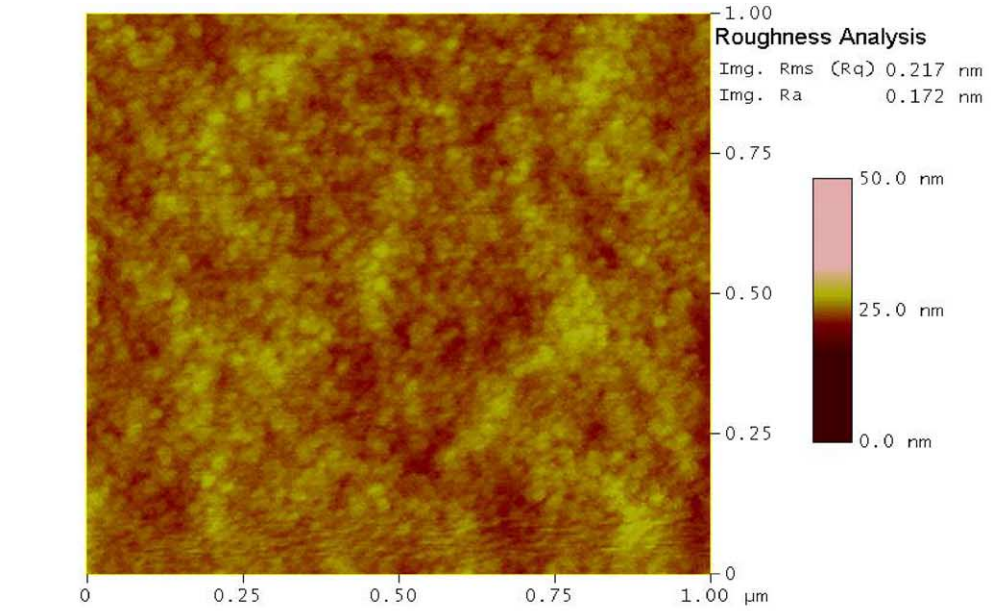

(a)

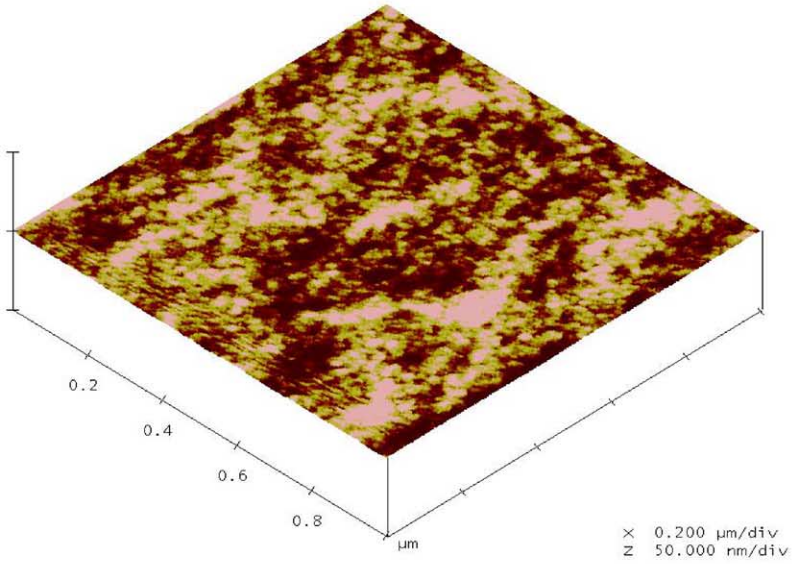

(b)

Fig. 5. The AFM images of TEOS/PHEMA hybrid gel containing 67 wt% TEOS. (a) Two-dimensional and (b) three-dimensional.

silica and PHEMA phases in the former and relatively stronger inter- and intra-molecular hydrogen bonding tethered the silica and PHEMA chains in the latter.

3.3. Surface morphology investigation

The AFM topographic images of colloidal silica/PHEMA and TEOS/PHEMA hybrid gels with colloidal silica and TEOS contents of 30 and 67 wt%, respectively, are shown in Figs. 4 and 5, respectively. The mean roughness (Ra) in the colloidal silica/PHEMA and TEOS/PHEMA films were 0.821 and 0.172 nm, respectively. In the AFM image, the bright region corresponded to higher friction, the silica phase, and the dark region to

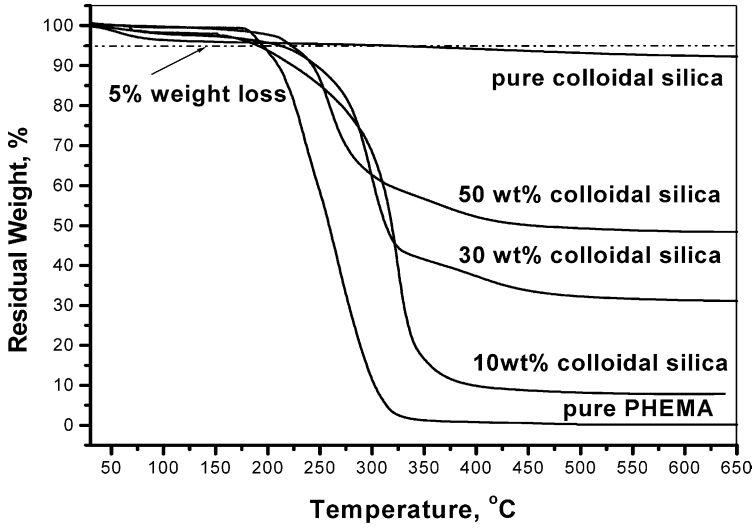

(a)

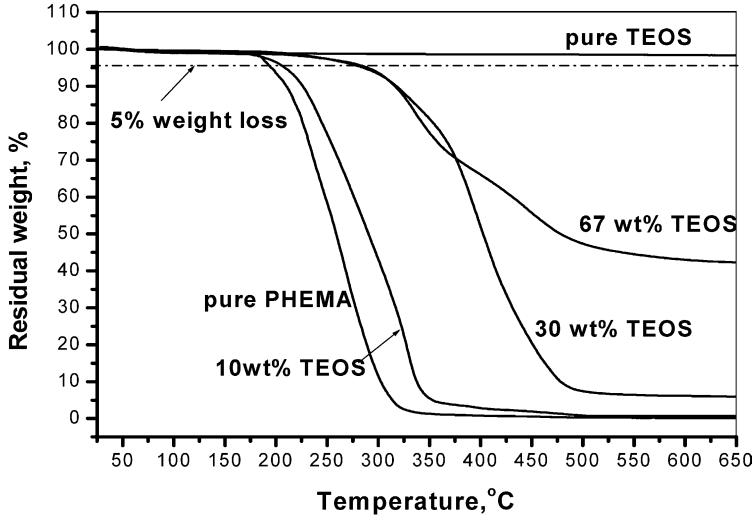

(b)

Fig. 6. TGA traces of (a) colloidal silica/PHEMA hybrid gels with various colloidal silica contents and (b) TEOS/PHEMA hybrid gels with various TEOS contents under HCl_{aq}-catalyzed condition.

the lower friction, the PHEMA phase. It was found that the boundaries between the silica and PHEMA phases were clearer with an oriented array of silica particles in the colloidal silica/PHEMA film surface, whereas, the boundaries between the silica and PHEMA phases were more ambiguous with random arrangement of silica particles in the TEOS/PHEMA film surface. This phenomenon provided further evidence that interfacial structures between silica and PHEMA phases in the colloidal silica/PHEMA and TEOS/PHEMA hybrids were different as discussed previously in the FT-IR spectra investigations.

3.4. Thermal and dynamic mechanical properties of the hybrids

The thermal decomposition behaviors of the dried hybrid gels were investigated by TGA at a heating rate of 10 °C/min under a nitrogen atmosphere as illustrated in Fig. 6. The temperature corresponding to 5 wt% loss was defined as the initial thermal degraded temperature of polymer phase, T_d. The T_d of pure PHEMA was at 200 °C and increased slightly with the addition of colloidal silica in the PHEMA, whereas, the T_d of TEOS/PHEMA hybrid gels significantly increased to above 300 °C when the content of

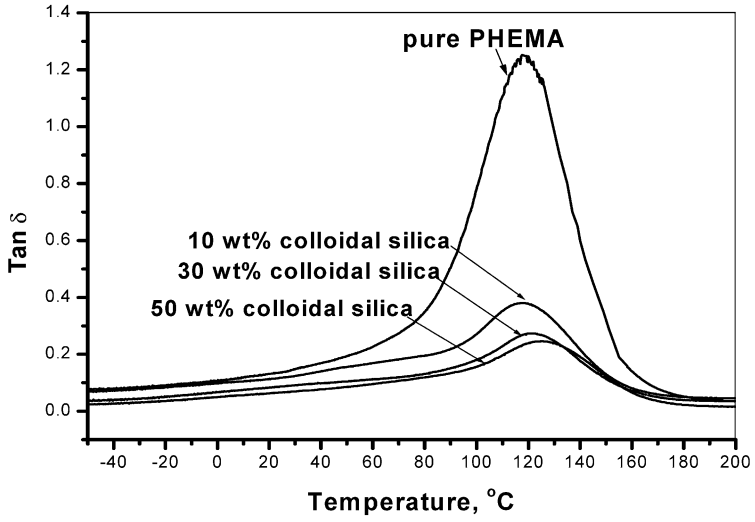

(a)

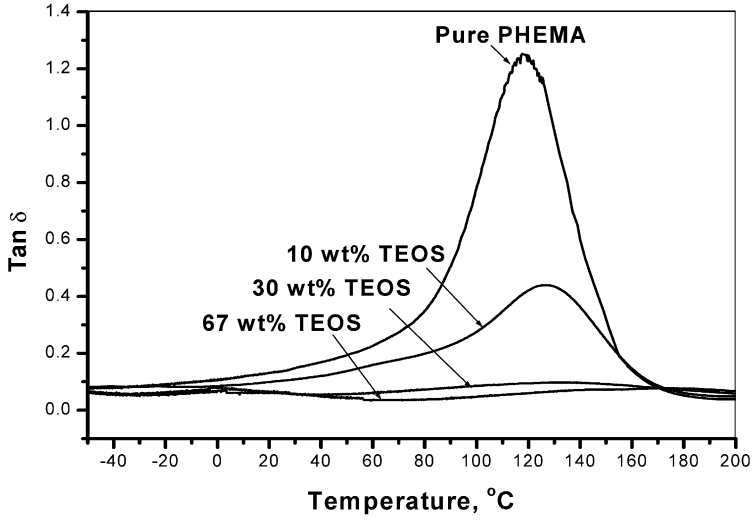

(b)

Fig. 7. Damping (tan δ) as a function of temperature of (a) colloidal silica/PHEMA hybrid gels with various colloidal silica contents and (b) the TEOS/PHEMA hybrid gels with various TEOS contents under HCl_{aq}-catalyzed condition.

TEOS in the sol was higher than 30 wt%. The silica content in the hybrid gel was found, according to the residual weight content at 650 °C in the TGA trace, to be slightly less than the original content of colloidal silica in the colloidal silica/PHEMA hybrid gel. Using pure TEOS to synthesis the silica, the yield was approach to 75 wt% after drying at 105 °C for 24 h. Based on this value to estimate the silica contents in the hybrids with TEOS content of 10, 30 and 67 wt%, were 7.5, 22.5, and 50.25 wt%, respectively. However, the residual weight contents of TEOS/PHEMA hybrids with TEOS content of 10, 30 and 67 wt% were 0.7, 6, and 42 wt%, respectively, as shown in Fig. 6b, which was significantly less than the theoretical estimated value. This result implies that the TEOS was only partially hydrolyzed and condensed to silica during the sol–gel process as the TEOS sol was mixed into the PHEMA/methanol solution. However, it is significant that although less silica formed in the TEOS/PHEMA hybrid gels they still exhibited better thermal resistance than the colloidal silica/PHEMA hybrid gels.

The difference in mechanical properties of the colloidal silica/PHEMA and TEOS/PHEMA hybrids can also be seen in the results of DMA. The damping (tan δ) and storage modulus (E') vs. the temperature of the colloidal silica/-PHEMA and TEOS/PHEMA hybrids are shown in Figs. 7 and 8, respectively. The damping peak of pure PHEMA

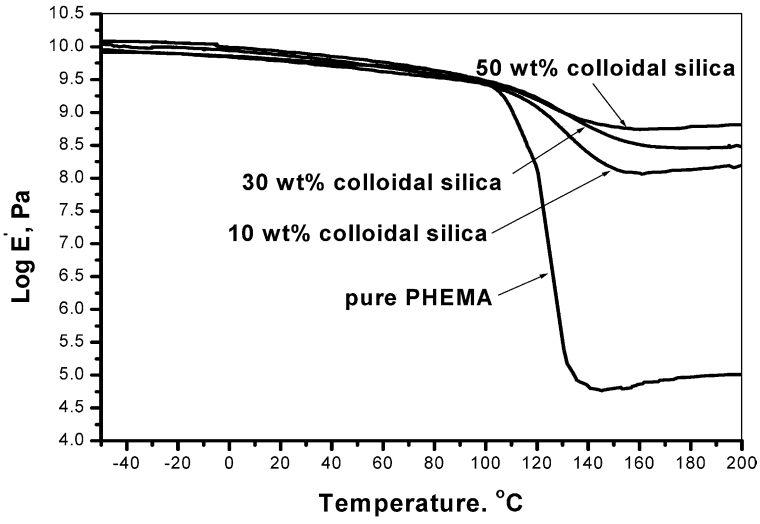

(a)

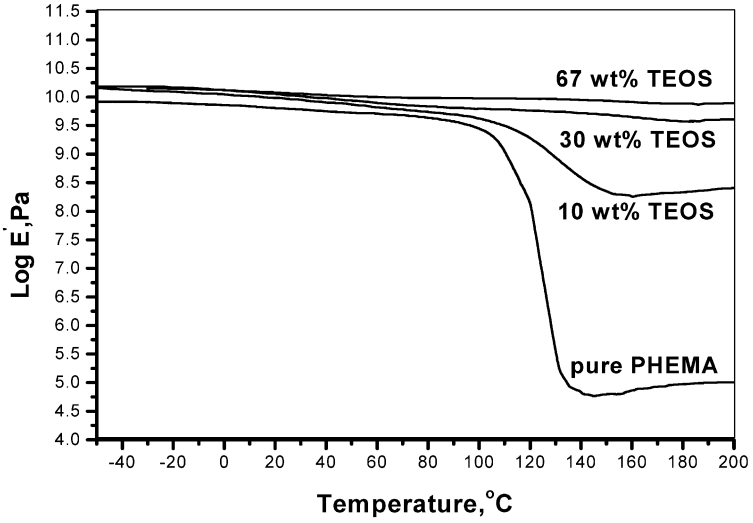

Fig. 8. Storage modulus (E') as a function of temperature of (a) colloidal silica/PHEMA hybrid gels with various colloidal silica contents and (b) the TEOS/PHEMA hybrid gels with various TEOS contents under HCl_{aq}-catalyzed condition.

occurred at 115 °C with a value of 1.25. When the colloidal silica was mixed with PHEMA, its damping peak proportionally decreased as the content of colloidal silica increased. The glassy state storage modulus of the colloidal silica/PHEMA hybrids remained almost the same as the pure PHEMA and the rubbery state storage modulus of the hybrid proportionally increased as the content of colloidal silica increased. In the TEOS/PHEMA hybrid with 10 wt% of TEOS content the damping was significantly reduced and the glassy state storage modulus was slightly higher than that of pure PHEMA. Moreover, the damping as well as the glassy transition became obscured as the TEOS content in the hybrid increased from 10 to over 30 wt%. The different behavior of these two hybrids during the dynamic loading provided more evidence for explaining the structural difference between the colloidal silica/PHEMA and the TEOS/PHEMA hybrids. In the former, colloidal silica uniformly dispersed in the PHEMA phases with slightly inter-molecular hydrogen bonding, whereas, in the latter, PHEMA chains extended into the nano-scale silica network with the inter- and intra-molecular hydrogen bonding tethering the silica and PHEMA chains.

Fig. 9 illustrates the thermal expansions behaviors of 30 wt% colloidal silica/PHEMA and 67 wt% TEOS/PHEMA hybrid films. An oriented array of silica particles in the colloidal silica/PHEMA film was observed as shown in Fig. 4; therefore, the thermal expansion behaviors in the colloidal silica/PHEMA film were different in the *x*- and *y*-directions. In the TEOS/PHEMA film, silica particles tethered with PHEMA chains with random distribution,

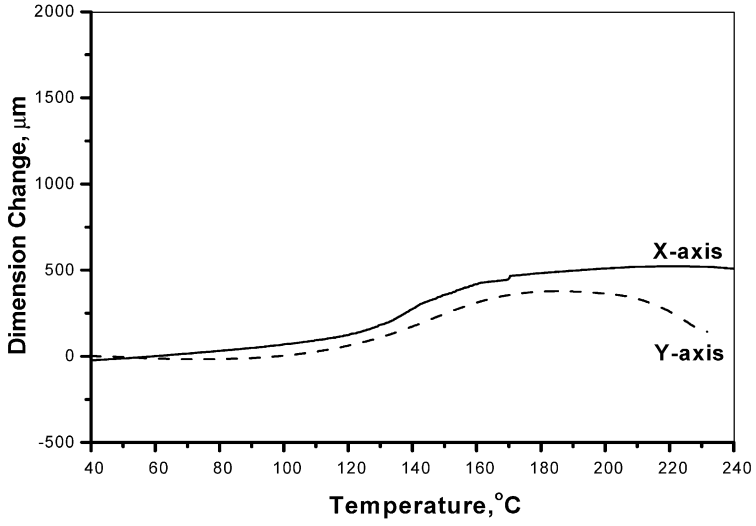

(a)

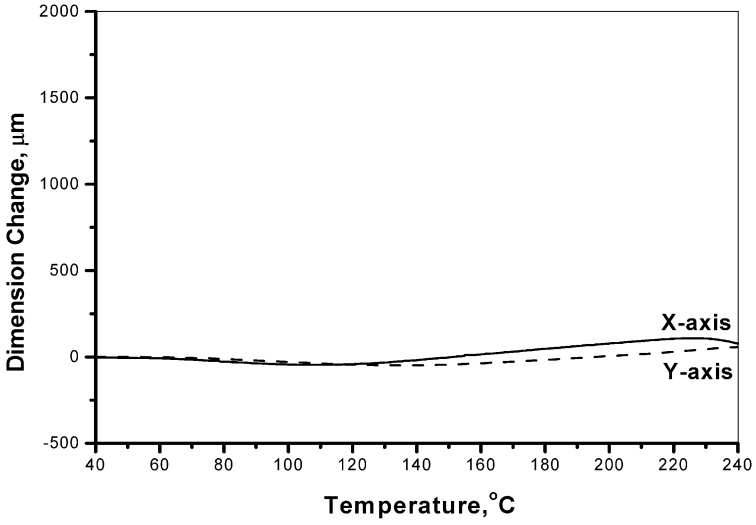

(b)

Fig. 9. Dimensional changes during heating of (a) 30 wt% colloidal silica/PHEMA hybrid gel and (b) 67 wt% TEOS/PHEMA hybrid gel.

hence, the thermal expansion behaviors of the film in the *x*- and *y*-directions were about the same.

3.5. The transmittance of hybrid gels

Fig. 10 shows the light transmittance of colloidal silica/PHEMA and TEOS/PHEMA hybrid gels. In the colloidal silica/PHEMA hybrid gels, the miscibility between PHEMA and silica particles decreased as the content of colloidal silica in the hybrid increased. At the low colloidal silica content of 10 wt%, the transmittance of the hybrid gel at the wavelength higher than 450 nm was even higher than the pure PHEMA. However, the transmittance of colloidal silica/PHEMA hybrid gel proportionally decreased as the content of colloidal silica further increased. One important factor that affected the light transmittance was the size of dispersed particles. The size of silica ranged from 3 to 70 nm in the 10 wt% colloidal silica/PHEMA hybrid and ranged from 2 to 250 nm in the 30 and 50 wt% colloidal silica/PHEMA hybrids, as shown in Fig. 1. Larger size and higher content of silica dispersed in the PHEMA matrix resulted with lower light transmittance of the hybrid gel. In the TEOS/PHEMA hybrid gels, the transmittance of hybrid gel was enhanced while the TEOS content increased. The transmittance of the hybrid gel was as high as 95% when the TEOS content increased to 67 wt%. Finer size of silica accompanying with the intra-molecular mixing

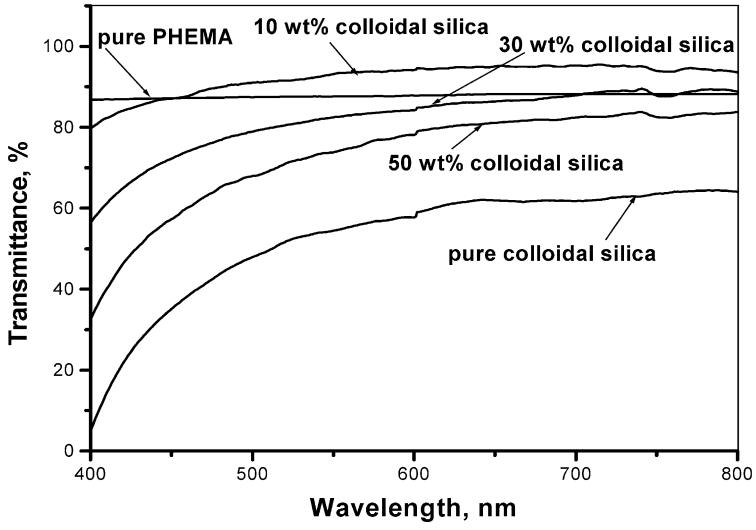

(a)

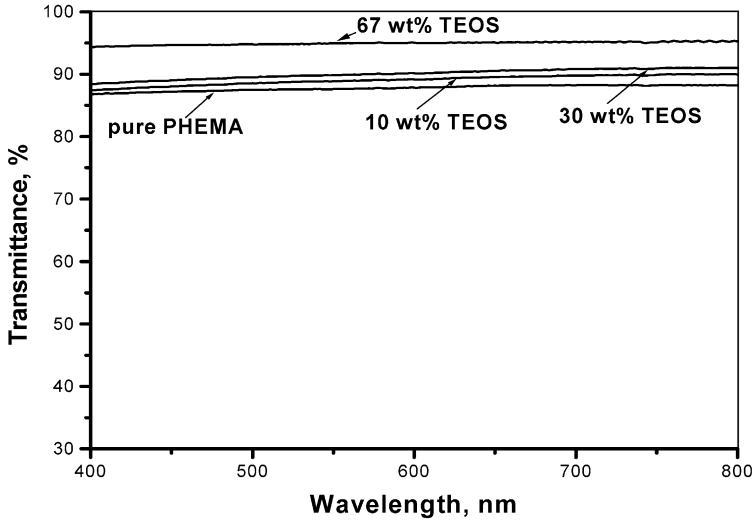

(b)

Fig. 10. Transmittance spectra of (a) colloidal silica/PHEMA gel with different colloidal silica contents and (b) TEOS/PHEMA hybrid gel with different TEOS contents.

between silica and PHEMA chains might be the reason to exhibit the superior light transmittance of TEOS/PHEMA hybrid gel.

4. Conclusions

The silica/PHEMA nanocomposites were prepared either by physically mixing colloidal silica and PHEMA or by mixing the TEOS precursor and PHEMA, followed by the sol–gel process. In the colloidal silica/PHEMA hybrids, the particle size of the silica ranged from 2 to 250 nm. In the TEOS/PHEMA hybrids, the major portion of growing silica particles ranged from 2 to 40 nm with a few particles growing and aggregating to a micrometer. In the colloidal silica/PHEMA hybrids, only slightly inter-molecular hydrogen bonding existed between the silica and PHEMA phases. On the other hand, in the TEOS/PHEMA hybrids the PHEMA chains extended into the nano-scale silica network with relatively stronger inter- and intra-molecular hydrogen bonding tethering the silica and PHEMA chains. Consequently, the TEOS/PHEMA hybrid gels, despite less silica being formed during the sol–gel process, exhibited a smoother surface and better thermal resistance and mechanical properties than the colloidal silica/PHEMA hybrid gels.

The transmittance of colloidal silica/PHEMA hybrid gel proportionally decreased as the content of colloidal silica increased. In the TEOS/PHEMA hybrid gels, the transmittance of the hybrid gel was enhanced while the TEOS content increased. The transmittance of the hybrid gel was as high as 95% when the TEOS content increased to 67 wt%.

Acknowledgements

We wish to thank the chemical system research division of the Chung-Shan Institute of Science and Technology (Taiwan) for partial financial support and supply of colloidal silica sol.

References

[1] Wang CJ, Pang Y, Prasad PN. Polymer 1991;32:605–8.
[2] Sung PH, Hsu TF. Polymer 1998;39:1453–9.
[3] Reyes-Esqueda J, Darracq B, Garcia-Macedo J, Canva M, Blanchard M, Chaput F, et al. Optics Commun 2001;198:207–15.
[4] Jeng RJ, Chang CC, Chen CP, Chen CT, Su WC. Polymer 2003;44: 143–55.
[5] Wang B, Wilkes GL, Hedrick JC, Liptak BC, McGrath JE. Macromolecules 1991;24:3449–59.
[6] Mackenzie JD, Huang Q, Iwamoto T. J Sol–gel Technol 1996;7: 151–9.
[7] Mark JE. Polym Eng Sci 1996;36:2905–13.
[8] Haas KH, Wolter H. Curr Opin Solid State Mater Sci 1999;4:571–80.
[9] Matejka L, Dukh O, Kolarik J. Polymer 2000;41:1449–59.
[10] Reetz MT. Adv Mater 1997;9:943–54.
[11] Ohsuki C, Miyazaki T, Tanihara M. Mater Sci Eng 2002;C22:27–34.
[12] Joseph R, Zhang S, Ford WT. Macromolecules 1996;29:1305–12.
[13] Motomatsu M, Takahashi T, Nie HY, Mizutani W, Tokumoto H. Polymer 1997;38:177–82.
[14] Huang ZH, Qiu KY. Polymer 1997;38:521–6.
[15] Guo L, Lee JH, Beaucage G. J Non-Cryst Solids 1999;243:61–9.
[16] Breiner JM, Mark JE, Beaucage G. J Polym Sci, Part B: Polym Phys 1999;37:1421–7.
[17] Hajji P, David L, Gerard JF, Pascault JP, Vigier G. J Polym Sci, Part B: Polym Phys 1999;37:3172–87.
[18] Ågren P, Counter J, Laggner P. J Non-Cryst Solids 2000;261: 195–203.
[19] Lin JM, Ma CCM, Wang FY, Wu HD, Kuang SC. J Polym Sci, Part B: Polym Phys 2000;38:1699–706.
[20] Costa ROR, Vasconcelos WL. J Non-Cryst Solids 2002;304:84–91.
[21] Habsuda GP, Simon YB, Cheng DG, Hewitt DA, Lewis HT. Polymer 2002;43:4123–36.
[22] Yu YY, Chen CY, Chen WC. Polymer 2003;44:593–601.
[23] Ji XL, Jiang SC, Qiu XP, Dong DW, Yu DH, Jiang BZ. J Appl Polym Sci 2003;88:3168–75.
[24] Brinker CJ, Scherer GW. Sol–gel science. vol. 1. New York: Academic Press; 1989 pp. 97–152.
[25] Novak BM, Ellsworth MW, Verrier C. In hybrid organic–inorganic composites. In: Mark JE, Lee CYC, Bianconi PA, editors. ACS Symposium Series 585. Washington, DC: American Chemical Society; 1995 (chapter 8).
[26] Huang SL, Chin WK, Yang WP. J Polym Sci, Part B: Polym Phys 2004;42:3476–86.
[27] Bosch P, Del Monte F, Mateo JL, Levey D. J Polym Sci, Part A: Polym Chem 1996;34:3289–96.